Ecological Engineering 57 (2013) 403–412

Contents lists available at SciVerse ScienceDirect

Ecological Engineering

journal homepage: www.elsevier.com/locate/ecoleng

Research paper

Estimation of N_2 and N_2O ebullition from eutrophic water using an improved bubble trap device☆

Yan Gao[a,1], Xinhong Liu[a,1], Neng Yi[b], Yan Wang[a], Junyao Guo[a], Zhenhua Zhang[a], Shaohua Yan[a,*]

[a] Institute of Agricultural Resources and Environment, Jiangsu Academy of Agricultural Sciences, 50 Zhongling Street, Nanjng 210014, China
[b] College of Resources and Environment Sciences, Nanjing Agricultural University, 1 Weigang Road, Nanjing 210095, China

ARTICLE INFO

Article history:
Received 24 October 2012
Received in revised form 1 April 2013
Accepted 7 April 2013

Keywords:
Nitrogen
Ebullition
Eutrophic
N_2
N_2O

ABSTRACT

Ebullition pathway of N_2 and N_2O emission and its importance on nitrogen loss were quantified during a survey of a eutrophic pond located at the subtropical climate zone in China. Using an improved bubble trap device, *in situ* collection of N_2 bubbles was achieved by avoiding the contamination of N_2 in the air. Measurements using the device indicated very high ebullition rates (36.3–366.7 ml m^{-2} h^{-1}) and N_2 ebullition flux (0.025–0.297 g m^{-2} h^{-1}) at warmer months of September and October. The ebullition rates and N_2 ebullition fluxes dropped sharply in colder months of December and January, ranged 2.5–15.9 ml m^{-2} h^{-1} and 0.002–0.016 g m^{-2} h^{-1}, respectively. Distinct spatial variation of ebullition rates, and N_2 and N_2O ebullition fluxes were observed, with the highest rate at the heavy sediment location. Ebullition of N_2O was a very minor fraction of total gaseous nitrogen released to air. The data demonstrated that ebullition could contribute greatly to biogenic N_2 fluxes in eutrophic waters with significant bubble emission.

1. Introduction

Aquatic eutrophication has led to a growing interest in processes that remove nitrogen from water (Pretty et al., 2003). Denitrification, the process of the microbial reduction of nitrate to gaseous nitrogen (dinitrogen N_2 and nitrous oxide N_2O), can remove a large proportion of nitrogen from water, and hence plays a critical role in buffering the impact of increased nutrient loads in aquatic ecosystems (Howarth and Marino, 2006; Seitzinger et al., 2006).

To quantify nitrogen loss in the process of denitrification in aquatic systems, rates of denitrification usually have been estimated in cores or the collected water and sediment samples (Saunders and Kalff, 2001; Zhong et al., 2010a). Most commonly, cores have been incubated in laboratories, and denitrification has been estimated by the acetylene inhibition (block) technique (Teissier and Torre, 2002; Zhong et al., 2010b). The acetylene inhibition method may dramatically underestimate denitrification rate, inhibits the nitrification process, and does not capture any coupled nitrification–denitrification (Seitzinger et al., 1993). Recently, ^{15}N isotope pairing method was developed to analyze the denitrification rates in the collected sediment core. The fundamental limitation of the isotope pairing method is of requiring a uniform mixture of the added $^{15}NO_3^-$ with the endogenous sources of $^{14}NO_3^-$ (Van Luijn et al., 1996). More recently, an open-channel N_2 approach was developed to analyze denitrification rate at the ecosystem scale based on the analysis of dissolved N_2 (N_2/Ar method) in the collected water samples on membrane inlet mass spectrometer (MIMS) (McCutchan et al., 2003). Precision for open-channel estimation of denitrification greatly depends on the amount of analytical error on measuring dissolved N_2 concentration in water samples. However, it does not necessarily catch nitrogen ebullitions, which come out to be an important source of nitrogen loss from aquatic ecosystems.

Laboratory experiments with sediment cores or the collected sediment and water samples may not fully simulate natural environment conditions. Therefore, *in situ* direct measurements of N_2 and N_2O emission are desirable.

There are at least four gas emission pathways in water bodies which may be regulated differently: ebullition flux, diffusive flux, storage flux, and flux through aquatic vegetation (Bastviken et al., 2004). Ebullition (bubbling) from sediments or whole water column was commonly observed in lakes and reservoirs (Delsontro et al., 2010). A recent gas analysis of the bubbles revealed that the

* Corresponding author. Tel.: +86 25 84390002; fax: +86 25 84391231.
E-mail address: shyan@jaas.ac.cn (S. Yan).

[1] These authors contributed equally to this work.

0925-8574/$ – see front matter © 2013 The Authors. Published by Elsevier B.V. All rights reserved.
http://dx.doi.org/10.1016/j.ecoleng.2013.04.020

bubbles consisted almost entirely of N_2 (Higgins et al., 2008). This suggested the importance of an alternative pathway for the flux of N_2 from aquatic systems to the atmosphere.

An inverted funnel is often deployed to trap methane bubbles from sediment since 1776 (Ferry and Kastead, 2007). Chanton et al. (1989) described a pyramid floating sampler to determine bubble fluxes from a tidal freshwater estuary. The Chanton's sampler had a syringe connected to its top *via* 5–10 m of 0.358-cm polypropylene tubing. Smith and Lewis (1992) used sealable plastic chambers with floating collar to measure methane bubbling in the Rockies, Colorado. At each sampling period, the Smith and Lewis' chambers were sealed, and the gas samples were removed through a septum with 5-cm^3 glass syringe equipped with three-way stopcocks. In another research project, similar devices were employed by Keller and Stallard in 1994 to trap methane bubbling from Gatun Lake, Panama City. In order to limit the moving of the devices in water, anchors were attached to the edge of the devices. Further more, luer fittings and a 20-gage hypodermic needle were connected to the top of the devices *via* a Tygon tube to facilitate gas sampling (Keller and Stallard, 1994). Later changes of a gas collecting and ebullition metering device were made by DeSutter and Ham in 2005. A gas sampling bag and exhaust pump were added to the DeSutter and Ham's device. Although gas collecting was motorized and the volume measuring was automatic, gas samples were collected manually (DeSutter and Ham, 2005). In recent years, similar method of collecting bubble gas, measuring its volume, sampling collected gas for various purposes, in separate steps, had been developed (Higgins et al., 2008; McLinn and Stolzenburg, 2009). The new device described in this paper makes the steps of collecting, measuring (in volume) and sampling gas ebullition automatic, fast, convenient, accurate and precise. Furthermore, the new device has advantages for estimating ebullition of N_2, which, otherwise, is difficult due to its high concentration in the air and could be easily contaminated.

In this study, an improved bubble trap device was used to automatically and continuously trap bubbles from water column and sediment in a eutrophic pond, Nanjing, Jiangsu Province, China. Using this device, *in situ* collection of N_2 bubbles can be achieved by avoiding the contamination of nitrogen in the air. Through direct analyzing of N_2 and N_2O concentration in the collected gas samples, N_2 and N_2O ebullition fluxes of water column and sediment will be further determined. It is expected that the present study could give an insight into the contribution of N_2 ebullition flux on nitrogen removal *via* denitrification in eutrophic water bodies.

2. Materials and methods

2.1. Study site

A eutrophic pond located at Jiangsu Academy of Agricultural Sciences (JAAS), Nanjing, China was selected in this study. The pond was constructed to store domestic wastewater and rain for rice field irrigation, with a sluice to control the water level. In China, such constructed pond is very popular in the countryside with the aim of field irrigation. The total nitrogen (TN) and the total phosphorus (TP) concentrations in the pond water have been higher than 2.0 mg l^{-1} and 0.2 mg l^{-1}, respectively, since 2000, which were worse than Grade V requirements according to Environmental Quality Standards for Surface Water of China (GB3838-2002) (SEPA, 2002). According to the standards, the water bodies are divided into five grades based on utilization purposes and protection objectives. The contamination is aggravated in the order Grade I < Grade II < Grade III < Grade IV < Grade V.

The pond has a surface area of ~5400 m^2 with a maximum depth of ~4 m at the center of the pond. The center channel going through the center of the pond contains less sediment because flushing discharge of water from the inlet, located at the northern side of the pond, washes away detritus and deposit. Aquatic macrophytes (*Eichhornia crassipes*) grew in confined enclosures in the pond beyond the sampling sites. Sediments consist mainly of clay, fine silt, leaves and contain about 2.5% organic carbon. In a temperate climate zone, the pond experiences seasonal water temperatures changing from ~5 °C in winter up to nearly 32 °C in summer. The average water residence time was ~1 month, with the shorter time in raining season and rice-growing season.

2.2. N_2 and N_2O ebullition study

The experiment was conducted from September 2011 to January 2012. N_2 and N_2O ebullition fluxes were assessed based on multiple sampling campaigns by trapping the bubbles by an improved bubble trap device. The detailed description of the device can be found in the following Section 2.3. The sampling points were shown in Fig. 1.

The water depth at the sampling points was 4 m (the center channel at pond center, location D1), 3.5 m (15 m away from the pond center, location D2) and 2.8 m (30 m away from the pond center, location D3). The different water depth at different sampling points was mainly of the consequence of different depth of sediment deposit at the pond bottom. The device, fixed by a rope to an anchor, was placed 5 m apart in line. Each depth had four replicates. We started to collect the samples at the D1, D2 and D3 sites from September onwards. The gas sampling duration was 24-h at each sampling time from September to October. The devices were setup at 8:00 a.m. in the morning, and the gas storage bottles were collected at 8:00 a.m. next morning. Each time the collected gas storage bottles (containing the gas samples) were replaced with new pre-filled bottles. In December, the gas sampling duration was extended to 1 week, and the duration was half a month in January. When collecting gas samples, the air temperatures were recorded twice a day, one at 8:00 a.m. and another at 15:00 p.m. At each sampling campaign, 1 l mixed water samples were collected from three depths (0–0.5 m, 1–1.5 m, and 0.5 m above the bottom) using a cylinder sampler to analyze NH_4^+, NO_3^-, TN and TP concentrations. The water samples were preserved with 0.5 ml of chloroform, and then kept in a refrigerator (~4 °C) until chemical analysis. Dissolved oxygen (DO) and pH at the upper water layer (0.5 m below the water surface) and bottom water layer (5 cm above the sediment) were monitored *in situ* simultaneously.

After dismounting the storage bottles, they were kept inverted and transported to lab. The volume of the collected gas in each bottle was determined by weighing the water loss. The ebullition rate was calculated using the following formula:

$$ER_i = (V/S/T) \times 273.15/(273.15 + t_i) \quad (1)$$

$$V = \frac{(W1 - W2)}{D} \quad (2)$$

where ER_i is ebullition rate of ml m^{-2} h^{-1} at standard temperature and pressure (STP); V is volume in ml; S is the dome mouth open area, m^2; T is duration of the time in h; t_i is the temperature at the time of measurement; $W1$ is the weight (g) of the pre-filled bottle at the start of the experiment; $W2$ is the weight (g) of the bottle after stay in the field over the length of duration.

D is the water density at the room temperature (g/ml) (McCutcheon et al., 1993),

$$D = 1 - \frac{(t + 288.9414)}{(508929.2 \times (t + 68.12963))} \times (t - 3.9863)^2,$$

$$0 \le t \le 50\,^{\circ}C$$

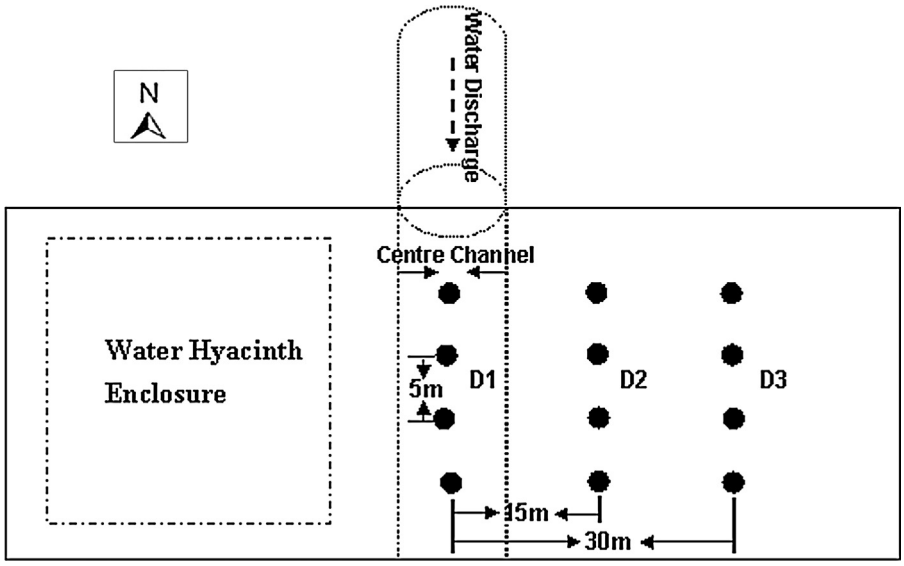

Fig. 1. Location of the sampling points in the pond. D1: sampling location D1 with water depth of ~4 m; D2: sampling location D2 with water depth of ~3.5 m; D3: sampling location D3 with water depth of ~2.8 m.

The collected bubble gas in the storage bottles was analyzed for N_2 and N_2O concentration. The N_2 and N_2O ebullition fluxes were calculated as follows:

$$E_{gas} = C_{gas} \times \rho_{gas} \times ER_i \quad (3)$$

where E_{gas} is the ebullition rate for N_2 or N_2O, in unit $g\,m^{-2}\,h^{-1}$; C_{gas} is the concentration of a specific gas; ρ_{gas} is the density of a specific gas at STP following the Ideal Gas Law, ρ (N_2) equal $1.25\,g\,l^{-1}$, $\rho(N_2O)$ equal $1.96\,g\,l^{-1}$.

2.3. Description of the improved bubble trap device

Gas ebullition is collected *via* a submerged floating dome. The dome was connected to an inversed storage bottle. The storage bottle was pre-filled with Milli-Q water. When gas accumulates in the dome, differential pressure, created by leveled drainage water gravity, forces the gas to continuously and automatically enter the inversed storage bottle, which measured the volume of gas, in consequence, the data being used for calculating ebullition rates and the collected gas in the storage bottle being used for analyzing its composition.

Fig. 2 provided a simple diagram of an exemplary version of the new device. An outlet dome tube 8 installed on the top of a dome 5 is connected to the inlet end of a two-way valve 6. The outlet end of the two-way valve 6 is connected to the inlet end of an intake latex tube 3. The outlet end of the inlet latex tube 3 is connected to the intake tube 9 of an inversed storage bottle 2 that is attached to string 15, which hung to a ring 16 on the top of an arc frame 1. The outlet tube 10 of the inversed storage bottle 2 is connected to one end of a drainage latex tube 4, and other end of the drainage latex tube 4 situated within water 14. The dome 5 was hung to rings 11 on the arc frame 1, *via* thread 12 attached to dome rings 7 on the dome 5. The arc frame 1 situated on floating balls 13 at the each corner of a square frame 17.

The floating frame is made of two galvanized iron thread, banded in a bow shape cross welded at 90 degrees. The frame height is 400 mm with a square shape bottom, at a length of 500 mm. The floating balls (100 mm in diameter) are made of enforced foam.

The polypropylene storage bottle (sample bottle) has a narrow neck sealed by a rubber stop. There were one intake tube (ø 6 mm) and one outlet tube (ø 6 mm) pierced through the rubber stop. The intake tube reaches the bottom of the bottle, and the outlet tube is of 8 mm in length. Both glass tubes extend 20 mm below the rubber stop of the inversed storage bottle.

The dome 5 also has a narrow necked top and a rubber stop, wherein the outlet dome tube 8 is installed. The open mouth inner diameter of the dome is 34.2 mm, and made of polypropylene. Its height is 19 mm. The two-way valve is made of nylon with connections (ø 6 mm) on both sides.

To operate the new device:

(1) Connect the device as described above, except the inversed storage bottle.
(2) Anchor the frame and dome to the ebullition site, then open the two-way valve, and fully submerge the dome under water until all the air in the dome and tube is evacuated then close the valve.
(3) Connect pure-water pre-filled inversed storage bottle to the intake and drainage latex tubes which is also filled with water and clamped at the end.
(4) Hang the inversed storage bottle to the top of the arc frame.
(5) Connect the two-way valve to the intake latex tube and then release the clamp.
(6) Put the water drainage latex tube within water and release the clamp.

Care should be taken not to trap any air bubbles in dome, tubes and bottle when connecting the device.

2.4. Checking the integrity and effectiveness of the bubble trap device

The integrity and effectiveness of the device were checked with a gas mixture (standard gas) of 15.5% N_2, 8.8% O_2, 43.3% CH_4, 2.01% CO_2 and $1\,\mu l\,l^{-1}$ N_2O, which was released into the dome under water. The concentration of the gas mixture was selected by following the average of gas composition data obtained in a pre-study in a local eutrophic pond. After 8 h, the two-way valve to the gas intake latex tube was connected to the top of the dome, and then, the gas in the dome was drawn into a pre-filled storage bottle following the standard sampling procedures. The recovery test had

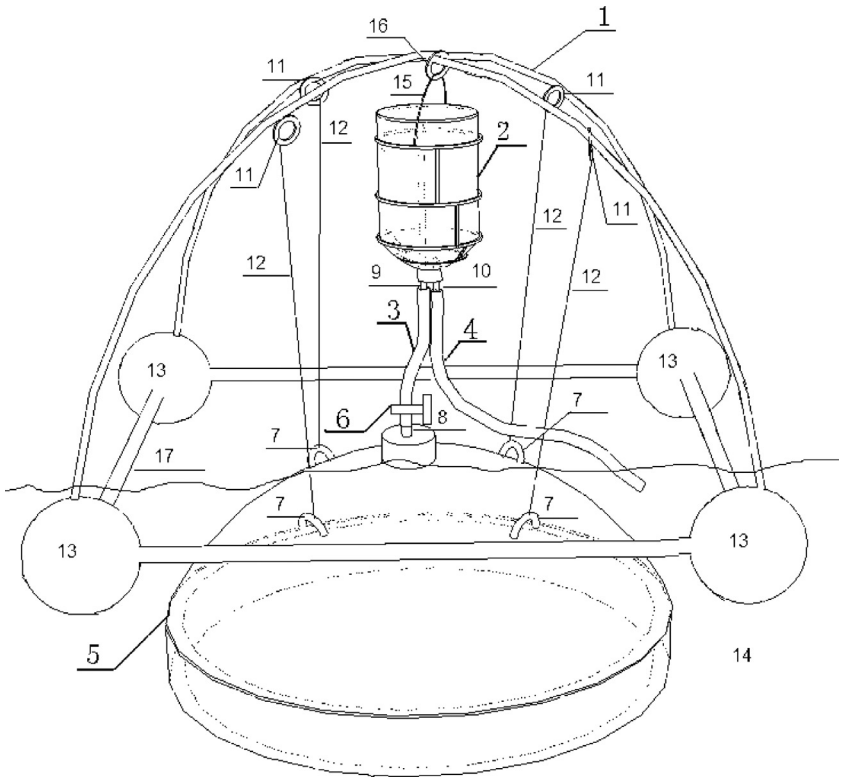

Fig. 2. Sketch of device for trapping and sampling ebullition.

four replicates. The volume of the collected gas in each storage bottle was immediately determined by weighing the water loss, and the concentration of each gas was analyzed using a GC with the methods described in the section of gas composition analysis section.

2.5. Partial pressure experiment

As nitrogen is an abundant element in nature with relatively high solubility in water (Pray et al., 1952), the effects of zero partial pressure in the head space of the sampling bottle at the start of the ebullition collection period was accessed with simulation experiment at the temperature from 20 °C to 30 °C and the air pressure at 7 m above the sea level. Nitrogen and oxygen saturated and sterilized water was prepared by adding 40 mol l^{-1} chlorine dioxide to one cubic meter of drinking water, and then, stirring the water continuously for two days with its surface opened to the air (Han et al., 2009), then the water being stabilizing for two days before experiment. The dome was immerged into the prepared water in a cubic container, and the device was set up in the laboratory according to the procedures described in the previous section. The sample bottle was pre-filled with Milli-Q water and collected after 7 days, which were chosen to cover enough length of duration practiced in the fields (usually the collection duration being less than three days). After sampling, the volume of the collected gas was determined according to the methods described in the above Section 2.2. The experiment was designed with four replicates.

2.6. Gas composition analysis

The sample bottles were kept inverted during sampling the bubbles and analyzing gas composition. During the analyses, the bottles were connected to a vacuum pump which drives the transfer of gas samples into the gas sampler of gas chromatograph (GC). In order to keep the pressure balance during the transfer of gas samples, the end of drainage latex tube on the mouth of the bottle was immerged beneath water. The end of an intake latex tube on the mouth of the bottle was connected to the vacuum pump. When certain volume of gas samples was transferred, equivalent volume of water was free flowing into the sample bottle.

N_2 was determined by using a gas chromatograph (GC-2014; Shimadzu Corporation) equipped with thermal-conductivity detector (TCD), molecular sievecolumn (Φ 3 mm × 2 m) and Ni63 electron capture detector (ECD), with highly purified He as the carrier gas (40 ml/min). When analyzing N_2 concentration, the temperature of column was 50 °C, and the temperature of detector was 100 °C, electrical current was at 80 mA. When analyzing N_2O concentration, the temperature of column was 65 °C, and the temperature of detector was 300 °C.

Qualitative analysis for both N_2 and N_2O was based on the retention time of the peak area of external standard method.

2.7. Other methods for analysis

Water temperature, pH, and DO were measured *in situ* by portable meter (YSI Pro Plus, USA) at the sample points. NH_4^+, NO_3^-, TN and TP were determined according to the Standard Methods (APHA, 2005).

2.8. Statistical analyses

The regression analyses between daily temperature and water ebullition rate at the different sampling sites in the pond were performed using Sigmaplot 12.0. The vertical box plot of temporal changes of N_2 and N_2O ebullition fluxes at the different locations of the pond were analyzed using Sigmaplot 12.0. The boundary of the box closest to zero indicated the 25th percentile, a solid line and a dash line within the box marked the median and mean,

Table 1
Recoveries of standard gases with known concentrations of N_2, O_2, CH_4 and N_2O.

	Specific gas			
	N_2	O_2	CH_4	N_2O
Standard gas concentration	15.5%	8.8%	43.3%	1 μl l^{-1}
Concentration in the collected gas samples	15.4 ± 0.3%	8.9 ± 0.04%	42.4 ± 0.7%	1.0 ± 0.02
Recovery of a specific gas	99.1 ± 0.8%	100.4 ± 0.5%	97.9 ± 1.7%	101 ± 2.2%

Recovery% = (concentration of a specific gas in the collected gas samples)/(standard gas with certain concentration of a specific gas) × 100.

respectively, and the boundary of the box farthest from zero indicated the 75th percentile. Whiskers (error bars) above and below the box indicated the 90th and 10th percentiles.

3. Results and discussion

3.1. Effectiveness and scientific significance of the improved bubble trap device

The recoveries of standard gases with fixed concentrations of N_2 (15.5%), O_2 (8.8%), CH_4 (43.3%) and N_2O (1 μl l^{-1}) were 99.1 ± 0.8% of N_2, 100.4 ± 0.5% of O_2, 97.9 ± 1.7% of CH_4, and 101 ± 2.2% of N_2O (Table 1). Precision for estimates of ebullition flux of individual gas (N_2, N_2O, O_2, CH_4 and CO_2) using the device mainly depends on the amount of analytical error in measurements of the collected gas concentration, but other factors are also important. Cares should be taken not to trap any air bubbles in dome, tubes and bottle when connecting the device, otherwise trapping bubbles will greatly bias analyses of individual gas concentration, especially for N_2 and O_2. This can be successfully achieved by filling dome, tubes and bottle with water. The sample bottles (gas sample storage bottles) were kept inverted during sampling the bubbles and analyzing gas composition. In this way, the water within the bottles would help to prevent the air entering into the bottle headspace. Through preventing air bubbles from entering into any components of the device, high recoveries of N_2 (99.1 ± 0.8%) was achieved when using the device to collect the standard gases. The dissolution of individual gas might influence the accuracy of the analyzable gas concentration in the storage bottle. This needs a further study.

The partial pressure experiment showed that the gas collected in the sample bottle over 7 days was 0.39 ± 0.22 ml, which was estimated at a rate of 0.024 ml per 12-h. This indicated that the release of the gas originally saturated in water was very minor when compared with the volume of gas released *via* ebullition, although solubility of N_2, O_2 and CO_2 was high.

Ideally, the device collected bubbles released from the water column (including sediment) beneath the mouth area of the dome. However, some bubbles released from sediment might be gradually dissolved during the movement along the water column, or be diverted by the wave current. This mainly depends on the dissolution of individual gas, the environmental parameters that influence the dissolution of the gas, e.g. the depth of water, hydrodynamic characteristics and the wind speed.

Ebullition is a common phenomenon observed in rivers, lakes, reservoirs, ponds and coastal ecosystems, especially on shallow (depth < 8 m) waters (Bastviken et al., 2004). In the shallow waters, the ebullition path is usually more effective than gas diffusion (DelSontro et al., 2011). As the eutrophic pond investigated in this study has a water depth of ~2.8–4 m, significant ebullition has been expected.

In the water with significant ebullition, measured gas flux could mainly result from bubble emission (Bastviken et al., 2004; Grinham et al., 2011). Keller and Stallard (1994) reported simultaneously determined average fluxes of methane by comparing the floating chamber (measuring both diffusive and ebullition fluxes) and bubble-trap method (only measuring the ebullition fluxes). Those two methods agreed reasonably well, given 97–98% of the measured flux resulted from bubble emissions. Compared with the floating chambers, the funnel bubble traps give a much more precise estimate of bubbling methane emission. Similarly, using the bubble trap method to study N_2 ebullition flux would lead to better understanding of nitrogen behavior in aquatic ecosystems with significant bubble emission. This is especially important in denitrification rate estimation.

It is difficult to estimate gaseous emission of nitrogen (N_2), no matter in diffusive way or ebullition way, due to high concentration of N_2 in the air. The device described in this paper provides a convenient and accurate way to *in situ* collect gaseous emission of N_2 released from water.

3.2. Water property during gas sampling campaigns

Dissolved oxygen (DO), pH, water temperature, nitrogen (NH_4^+, NO_3^-, TN) and TP concentrations were monitored during the gas sampling campaigns (September 2011 to January 2012) (Table 2). DO values ranged 7.6 ± 0.2–12.5 ± 1.2 at the upper water layer (0.5 m below the water surface), and 1.9 ± 0.7–7.5 ± 0.2 at the bottom water layer (5 cm above the sediment) from September 2011 to January 2012. In September and October, DO concentrations at the upper water layer were much higher ($p < 0.01$)

Table 2
Water property during the gas sampling campaigns.

Items		2011 September	2011 October	2011 December	2012 January
DO (mg l^{-1})	Upper water layer	12.5 ± 1.2	11.8 ± 1.1	8.4 ± 0.3	7.6 ± 0.2
	Bottom water layer	3.0 ± 0.4	1.9 ± 0.7	7.5 ± 0.2	7.3 ± 0.4
pH	Upper water layer	7.8 ± 0.1	7.5 ± 0.2	7.1 ± 0.1	6.9 ± 0.1
	Bottom water layer	6.9 ± 0.2	7.0 ± 0.2	7.0 ± 0.1	6.9 ± 0.1
Water temperature (°C)	Upper water layer	22.5 ± 2.0	20.1 ± 1.5	6.5 ± 0.5	4.9 ± 0.7
	Bottom water layer	21.6 ± 1.5	20.0 ± 1.4	7.0 ± 0.5	5.6 ± 0.6
NH_4^+ (mg l^{-1})	Mixed water samples	0.7 ± 0.1	0.6 ± 0.1	3.1 ± 0.4	3.2 ± 0.1
NO_3^- (mg l^{-1})	Mixed water samples	2.6 ± 0.7	2.9 ± 0.6	1.2 ± 0.4	0.4 ± 0.1
TN (mg l^{-1})	Mixed water samples	5.9 ± 0.7	5.8 ± 1.0	6.1 ± 1.2	5.6 ± 0.6
TP (mg l^{-1})	Mixed water samples	0.42 ± 0.11	0.51 ± 0.20	0.28 ± 0.06	0.32 ± 0.12

Upper water layer: 0.5 m below the water surface. Bottom water layer: 5 cm above the sediment. Mixed water samples: water samples collected from three depths (0–0.5 m, 1–1.5 m, and 0.5 m above the bottom).

Table 3
The ebullition rate of the pond water at the different months.

Ebullition rate ($ml\,m^{-2}\,h^{-1}$)		2011 September	2011 October	2011 December	2012 January
30 m	Mean ± SD	217.1 ± 73.4	172.0 ± 56.4	11.8 ± 3.2	6.4 ± 2.0
	Median	217.0	162.4	11.4	5.6
	Minimum	77.7	73.7	7.4	4.7
	Maximum	366.7	269.2	15.9	9.9
15 m	Mean ± SD	–	108.6 ± 41.6	6.8 ± 3.3	5.5 ± 1.5
	Median	–	94.4	5.7	5.4
	Minimum	–	64.7	3.8	3.9
	Maximum	–	221.3	14.0	7.3
0 m	Mean ± SD	136.3 ± 52.0	86.8 ± 39.0	5.5 ± 1.9	3.0 ± 0.4
	Median	145.5	76.3	5.1	3.0
	Minimum	36.3	47.2	9.3	2.5
	Maximum	217.9	177.3	3.9	3.5

30 m: 30 m away from the center channel, sampling location D3 with water depth of ~2.8 m;
15 m: 15 m away from the center channel, sampling location D2 with water depth of ~3.5 m;
0 m: the center channel, sampling location D1 with water depth of ~4 m;
Mean ± SD: September, $n = 40$; October, $n = 44$; December, $n = 12$; January, $n = 8$.

than values at the bottom water layer. The lowest DO values ($1.9 \pm 0.7\,mg\,l^{-1}$) were detected at the bottom water layer in October. The pH values ranged 6.9 ± 0.1–7.8 ± 0.1. Water temperature ranged 4.9 ± 0.7–22.5 ± 2.0 at upper water layer, and 5.6 ± 0.6–21.6 ± 1.5 at bottom layer from September 2011 to January 2012. The concentrations of TN in the pond water ranged 5.6 ± 0.6–$6.1 \pm 1.2\,mg\,l^{-1}$. The NH_4^+ concentrations in the pond water in September and October (0.7 ± 0.1 and $0.6 \pm 0.1\,mg\,l^{-1}$, respectively) were much lower than those in December and January (3.1 ± 0.4 and $3.2 \pm 0.1\,mg\,l^{-1}$, respectively), while NO_3^- concentrations in the pond water in September and October (2.6 ± 0.7 and $2.9 \pm 0.6\,mg\,l^{-1}$, respectively) were much higher than those in December and January (1.2 ± 0.4 and $0.4 \pm 0.1\,mg\,l^{-1}$, respectively). The TP concentrations in the pond water ranged 0.28 ± 0.06–$0.51 \pm 0.20\,mg\,l^{-1}$.

3.3. Ebullition rate in the eutrophic pond

In this study, the eutrophic pond located at the subtropical climate zone in China was observed for abundant ebullition in warmer months (September and October), which can be up to $366.7\,ml\,m^{-2}\,h^{-1}$ (Table 3). The average ebullition rates in September and October were $136.3 \pm 52.0\,ml\,m^{-2}\,h^{-1}$ and $86.8 \pm 39.0\,ml\,m^{-2}\,h^{-1}$ at the pond center (location D1), respectively, which were much higher than these in December and January. At the location D2 and D3, the ebullition rates showed a similar temporal changing pattern. Bubble ebullition has been identified as a major process in the release of gases from organic-rich and anoxic freshwater sediments to the water column and then to the atmosphere (Chanton and Whiting, 1995). As the autumn (September and October) approached, the increase in the ebullition in the pond was associated probably with the increased temperature and/or sedimentation (Chanton and Whiting, 1995; Joyce and Jewell, 2003), which supplied fresh organic material for bubble production until temperature decreased. High organic carbon content of sediment combined with warm temperatures support high rates of ebullition (Pribyl et al., 2005; McCutchan and Lewis, 2008). In this study, the organic matters in sediment mainly came from sewage sludge and detritus of water hyacinth (*E. crassipes*), and had higher organic carbon content of 2.5%. The air temperature ranged 18–34 °C, and water temperature ranged 15–28 °C from September to October. All of these conditions supported the abundant bubbles from the pond water. An increase in the ebullition during a summer period for eutrophic Lake Suwa (Japan) or during an autumn period for Lake Postilampi (Philand) has been reported (Takita and Sakamoto, 1993; Huttunen et al., 2001). Cold temperatures decreased the ebullition rates of the pond water. In the cold winter (December and January), the ebullition rates in the eutrophic pond dropped sharply, ranged from 2.5 to $15.9\,ml\,m^{-2}\,h^{-1}$ (Table 3).

Temperature seems being one of the major environmental factors that drive the changes of ebullition rates. In addition to above temperature-driven monthly decrease of ebullition rates, the fluctuation of the daily ebullition rates in the ponds was observed in September and October, which was in consistence with the fluctuation of daily air temperature (Fig. 3). Significant correlations between changes of daily temperature and water ebullition rates at the different sampling sites in the pond have been revealed (Fig. 4). In addition to affecting the biological reactions that could produce gases in water and sediment (Amatya et al., 2009), the changes of air temperature in warm seasons were more related with the changes of lighting intensity that directly affects the gas production *via* photosynthesis of phytoplankton (MacIntyre et al., 2000). In the warm months, bloom of phytoplankton was a common phenomenon observed in eutrophic water body. When air temperature decreased and cloudy day came, the photosynthesis of phytoplankton was correspondingly reduced and thereby the gas ebullition decreased.

In the same month, the medium ebullition rates were in the order of location D3 > location D2 > location D1. The spatial variation of ebullition rate seems related to the variation of the depth of sediment deposit at the pond bottom. The sediment layer was of the thinnest at the channel center where wastewater was flushed through, which resulted in the lowest ebullition rate. Correspondingly, the highest rates were observed at the sampling location where sediment layer was the deepest. As sediment was the main source of bubbling gas (Brennwald et al., 2005), it was reasonable to expect higher ebullition rates in location with heavier sediment. Moreover, the heavier sediment was accompanied by shallower water depth in this study. A previous study indicated that ebullition was in dependence on water depth, and 25–80% of ebullition was in locations where water depths were 4 m or less. In deeper waters, ebullition occurred was less than 10% of the chambers that were used to collect bubbles (Bastviken et al., 2004).

3.4. N_2 ebullition flux

In the previous studies, diffusive flux of N_2 was assumed to be the significant pathway for N_2 transport from water column to the atmosphere (Laursen and Seitzinger, 2002a; Hamersley and Howes, 2005). This study suggested that ebullition could contribute greatly

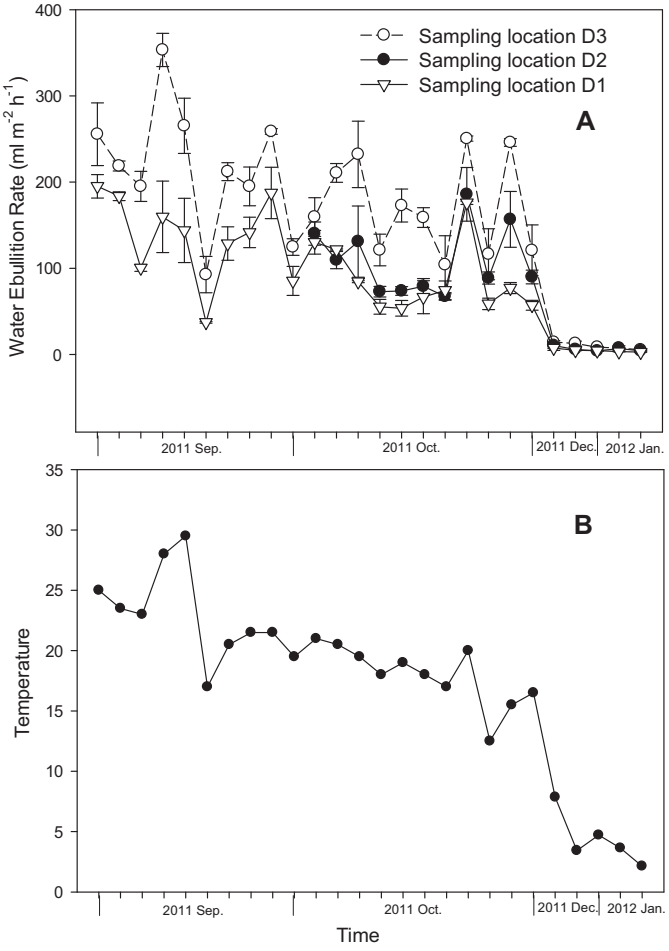

Fig. 3. Daily changes of the ebullition rate (A) of the pond water and air temperature °C (B). Sampling location D3: 30 m away from the pond center; Sampling location D2: 15 m away from the pond center; sampling location D1: the pond center.

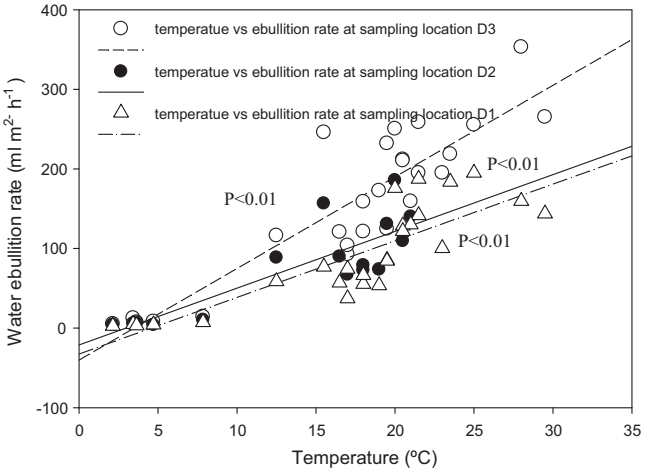

Fig. 4. Correlations between changes of daily temperature and water ebullition rate at different sampling sites. Sampling location D3: 30 m away from the pond center; Sampling location D2: 15 m away from the pond center; sampling location D1: the pond center.

Table 4
Comparison of N_2 ebullition rate with reference data.

Aquatic type and location	Denitrification ($g\,N\,m^{-2}\,h^{-1}$)	References
Subtropical Pond, East China	September 2011: 0.061 ± 0.024 October 2011: 0.12 ± 0.058	This study
Juilong River, South China	July 2010: 0.014 ± 0.007	Fredriksson (2010)
South Platte River	April 2000–October 2001: 0.086 ± 0.013	Pribyl et al. (2005)
Changjiang River	October 2002: 0.039 ± 0.017 March 2003: 0.080 ± 0.041	Yan et al. (2004)
Iroquois River	June 1999: 0.048 ± 0.018 May 2000: 0.118 ± 0.058	Laursen and Seitzinger (2002a)
Sugar Creek	May 2000: 0.004 ± 0.017	
Millstone River	March 2001: 0.221 ± 0.035	
South Platte River	November 1998: 0.110 ± 0.002	McCutchan et al. (2003)

to transportation of the biogenic N_2 from sediment to water column and then to the atmosphere. At warmer seasons of September and October, the average N_2 ebullition flux of the pond water ranged from $0.051 \pm 0.018\,g\,m^{-2}\,h^{-1}$ to $0.157 \pm 0.065\,g\,m^{-2}\,h^{-1}$. The average N_2 ebullition fluxes in September and October were $0.051 \pm 0.018\,g\,m^{-2}\,h^{-1}$ and $0.083 \pm 0.040\,g\,m^{-2}\,h^{-1}$, respectively, at the pond center (location D1) (Fig. 5). These were of up-middle level when compared with other studies using the open-channel estimation based on the measurement of dissolved N_2 in water (Table 4). The open-channel estimation only considers the diffusive path of N_2. The comparison of our results with these published data suggested that further comprehensive studies are needed in consideration of more accurate estimation of denitrification rate, especially for the water body with obvious ebullition.

Ebullition has been identified as a major process for the transport of CH_4 and CO_2 through the sediment/water interface (Ostrovsky, 2003). Sediment is a major site in aquatic ecosystem where denitrification and carbon decomposition occur simultaneously. During the mineralization of organic matter in sediments, a major portion of the mineralized nitrogen is lost from the ecosystem *via* denitrification. N_2 fluxes accounted for 76–100% of the sediment-water nitrogen flux in rivers and lakes and 15–70% in estuarine and coastal marine sediments (Seitzinger, 1988). Bubbles were formed in the sediment when the sum of the partial pressures of dissolved sediment gases exceeds the hydrostatic pressure (Brennwald et al., 2005). The bubbles, consisting mainly of CH_4, nitrogen N_2, and carbon dioxide CO_2, may be released from the sediment through the water column to the atmosphere either spontaneously, or this can be triggered by some episodic events such as changes in air pressure, hydrostatic pressure and wind activity (Mattson and Likens, 1990; Huttunen et al., 2001).

Flux of N_2 ebullition also varied seasonally (Fig. 5). These fluxes were greatly higher than these observed in December 2011 to January 2012 ($0.004 \pm 0.002\,g\,m^{-2}\,h^{-1}$). At the location D2 and D3, the N_2 ebullition fluxes in September and October were also significantly ($p < 0.05$) higher than that in December 2011 to January 2012. Seasonal variation of denitrification rates in sediment and waters has been commonly observed in previous studies (Poulin et al., 2007; Tortosa et al., 2011), which may led to different N_2 ebullition flux and diffusive flux. Another interesting phenomena observed in our study was that N_2 ebullition fluxes observed in October were higher than those in September. The primary factor influencing the denitrification rate was DO, and followed by temperature (Cornwell et al., 1999). The lowest DO concentrations ($1.90 \pm 0.71\,mg\,l^{-1}$) were observed at the bottom water layer (5 cm above the sediment) of the pond in October, when compared

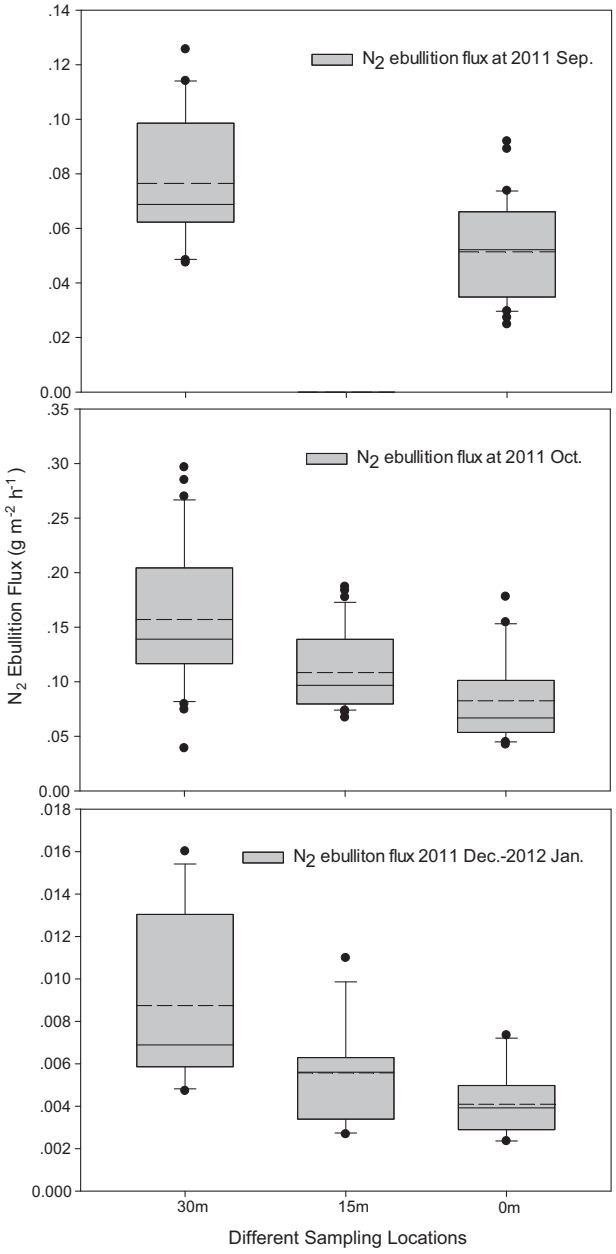

Fig. 5. Temporal changes of N_2 ebullition fluxes at the different locations of the pond. 30 m: 30 m away from the pond center, sampling location D3; 15 m: 15 m away from the pond center, sampling location D2; 0 m: the pond center, sampling location D1.

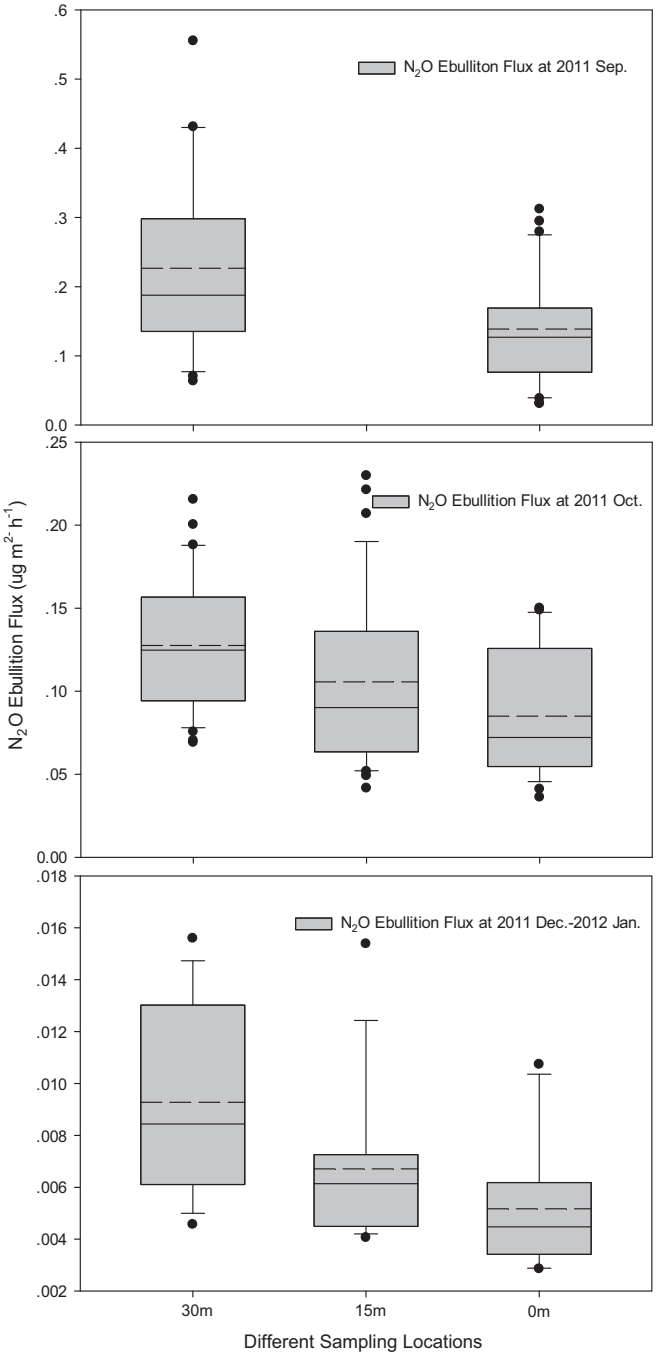

Fig. 6. Temporal changes of N_2O ebullition fluxes at the different locations of the pond. 30 m: 30 m away from the pond center, sampling location D3; 15 m: 15 m away from the pond center, sampling location D2; 0 m: the pond center, sampling location D1.

with other months (Table 2). As low DO condition supported high denitrification rates in sediment or sediment-water surface, it is reasonable to expect that N_2 ebullition fluxes in October were higher than that in September.

Distinct spatial variation of N_2 ebullition flux was also observed, with the highest rates at the heavy sediment location. In the same month, both the average and medium N_2 ebullition fluxes were in the order of location D3 > location D2 > location D1 (Fig. 5). This may lead to re-thinking of restoration strategies to improve water quality using sediment dredging (Gustavon et al., 2008; Zhong et al., 2010b) and sediment curing (Murphy et al., 1999). Sediment was believed to be the major sources of denitrification and therefore could have the vital influence on the biogenic N_2 ebullition flux and diffusive flux, hence to release the nitrogen in the aquatic systems (Laursen and Seitzinger, 2002b). Spatial variation of denitrification in sea and river has also been observed in previous studies (Pattinson et al., 1998; Chang and Devol, 2009).

3.5. N_2O ebullition flux in the eutrophic pond

Ebullition of N_2O was a very minor fraction of total nitrogen released to the air in this study. The highest average N_2O ebullition flux observed among different months was $0.27 \pm 0.14\ \mu g\ m^{-2}\ h^{-1}$, which was only million-digit-order less than in the form of N_2 flux. This is consistent with other studies that N_2 was

the major products of denitrification from diffusive path in aquatic ecosystem and N_2O was a very minor fraction (mostly $N_2O/N_2 < 1/100$) (Cole and Caraco, 2001; Beaulieu et al., 2011). N_2O ebullition flux also varied both spatially and seasonally. The average N_2O ebullition fluxes in September and October were $0.138 \pm 0.078\ \mu g\ m^{-2}\ h^{-1}$ and $0.0085 \pm 0.038\ \mu g\ m^{-2}\ h^{-1}$, respectively, at the center channel (location D1) (Fig. 6). These fluxes were obviously higher than that observed in December 2011 to January 2012 ($0.0052 \pm 0.0024\ \mu g\ m^{-2}\ h^{-1}$). The average N_2O ebullition fluxes in September and October at location D2 and D3 were also obviously higher than that observed in December 2011 to January 2012 (Fig. 6).

The importance of N_2O release may be in the considerations of greenhouse effect. N_2O has an effective index of 288 than CO_2 (IPCC, 2006). The processes of N_2O release have not been well understood, especially on its related environmental characteristics, such as DO, microbial and nutrient conditions. For ecosystem restoration and environmental protection, less N_2O release and maximize N_2 release are both desirable. To achieve these, more detailed researches on the nitrogen cycle and its behaviors in aquatic ecosystems are needed.

4. Conclusion

The improved bubble trapping device described here provides an alternative method to *in situ* estimate nitrogen loss *via* denitrification from aquatic ecosystems with significant ebullition. Using the device, *in situ* collection of N_2 bubbles has been achieved by avoiding the contamination of N_2 in the air. In the eutrophic pond located at the subtropical climate zone in China, ebullition rates and N_2 ebullition fluxes were very high at warmer months of September and October, and dropped sharply in colder months of December and January. Distinct spatial variation of ebullition rate, and N_2 and N_2O ebullition fluxes were observed, with the highest rates at the heavy sediment location. Ebullition of N_2O was a very minor fraction of total gaseous nitrogen released to air. All of these results demonstrated that ebullition could contribute greatly to biogenic N_2 fluxes in eutrophic waters with significant bubble emission.

Acknowledgments

The authors are grateful for the financial support from State Natural Science Foundation of China (No. 31100373), and "973" Special Preliminary Study Program (No. 2012CB426503).

References

Amatya, I.M., Kansakar, B.R., Tare, V., Fiksdal, L., 2009. Impact of temperature on biological denitrification process. J. Inst. Eng. 7, 121–126.
APHA, 2005. Standard Methods for the Examination of Water and Wastewater, 18th ed. American Public Health Association, American Water Works Association, Water Environment Federation, Washington.
Bastviken, D., Cole, J., Pace, M., Tranvik, L., 2004. Methane emissions from lakes: dependence of lake characteristics, two regional assessments, and a global estimate. Global Biogeochem. Cycles 18, GB4009.
Beaulieu, J.J., Tank, J.L., Hamilton, S.K., Wollheim, W.M., Hall Jr., R.O., Mulhollande, P.J., Peterson, B.J., Ashkenas, L.R., Cooper, L.W., Dahm, C.N., Dodds, W.K., Grimm, N.B., Johnson, S.L., McDowell, W.H., Poole, G.C., Valett, H.M., Arango, C.P., Bernotr, M.J., Burgin, A.J., Crenshaw, C.L., Helton, A.M., Johnson, L.T., O'Brien, J.M., Potter, J.D., Sheibley, R.W., Sobota, D.J., Thomas, S.M., 2011. Nitrous oxide emission from denitrification in stream and river networks. Proc. Natl. Acad. Sci. USA 108, 214–219.
Brennwald, M.S., Kipfer, R., Imboden, D.M., 2005. Release of gas bubbles from lake sediment traced by noble gas isotopes in the sediment pore water. Earth Planet. Sci. Lett. 235, 31–44.
Chang, B.X., Devol, A.H., 2009. Seasonal and spatial patterns of sedimentary denitrification rates in the Chukchi sea. Deep-Sea Res. Pt. II 56, 1339–1350.
Chanton, J.P., Marten, C.S., Kelley, C.A., 1989. Gas transport from methane-saturated, tidal freshwater and wetland sediment. Limnol. Oceanogr. 34, 807–819.
Chanton, J.P., Whiting, G.J., 1995. Trace gas exchange in freshwater and coastal marine environments: ebullition and transport by plants. In: Matson, P.A., Harriss, R.C. (Eds.), Biogenic Trace Gases: Measuring Emissions from Soil and Water. Blackwell Science, Oxford, pp. 98–125.
Cole, J.J., Caraco, N.F., 2001. Emissions of nitrous oxide (N_2O) from a tidal, freshwater river, the Hudson River, New York. Environ. Sci. Technol. 35, 991–996.
Cornwell, J.C., Kemp, W.M., Kana, T.M., 1999. Denitrification in coastal ecosystems: methods, environmental controls, and ecosystem level controls, a review. Aquat. Ecol. 33, 41–54.
DelSontro, T., Kunz, M.J., Kempter, T., Wüest, A., Wehrli, B., Senn, D.B., 2011. Spatial heterogeneity of methane ebullition in a large tropical reservoir. Environ. Sci. Technol. 45, 9866–9873.
Delsontro, T., Mcginnis, D.F., Sobeck, S., Ostrovsky, I., Wehrl, B., 2010. Extreme methane emissions from a Swiss hydropower reservoir: contribution from bubbling sediments. Environ. Sci. Technol. 44, 2419–2425.
DeSutter, T.M., Ham, J.M., 2005. Lagoon-biogas emissions and carbon balance estimates of a swine production facility. J. Environ. Qual. 34, 198–206.
Ferry, J.G., Kastead, K.A., 2007. Methanogensis. Molecular and Cellular Biology. ASM Press, Washington, DC (Chapter 13).
Fredriksson, C., 2010. Denitrification Rates in the Jiulong River in South East China. Research Report International Summer Water Resources Research School. Xiamen University, Xiamen, China.
Grinham, A., Dunbabin, M., Gale, D., Udy, J., 2011. Quantification of ebullitive and diffusive methane release to atmosphere from a water storage. Atmos. Environ. 45, 7166–7173.
Gustavon, K., Burton, G.A., Francingues, N.R., Reible, D., Vorhees, D.J., Wolfe, J.R., 2008. Evaluating the effectiveness of contaminated-sediment dredging. Environ. Sci. Technol. 42, 5042–5047.
Hamersley, M.R., Howes, B.L., 2005. Evaluation of the N2 flux approach for measuring sediment denitrification. Estuar. Coast. Shelf Sci. 62, 711–723.
Han, Y.B., Zhang, J.H., Peng, L., Lu, G.N., Gan, Y.X., Li, H., Chen, T., 2009. Experimental observation on germicidal efficacy and toxicity of a stable chlorine dioxide disinfectant. Chin. J. Disinfect. 26, 621–623.
Higgins, T.M., McCutchan Jr., J.H., Lewis Jr., W.M., 2008. Nitrogen ebullition in a Colorado plains river. Biogeochemistry 89, 367–377.
Howarth, R.W., Marino, R.M., 2006. Nitrogen as the limiting nutrient for eutrophication in coastal marine ecosystems: evolving views over 3 decades. Limnol. Oceanogr. 51, 364–376.
Huttunen, J.T., Lappalainen, K.M., Saarijärvi, E., Väisänenc, T., Martikainen, P.J., 2001. A novel sediment gas sampler and a subsurface gas collector used for measurement of the ebullition of methane and carbon dioxide from a eutrophied lake. Sci. Total Environ. 266, 153–158.
IPCC, 2006. Guidelines for national greenhouse gas inventories. In: Eggleston, S., Buendia, L., Miwa, K., Ngara, T., Tanabe, K. (Eds.), Intergovernmental Panel on Climate Change. Institute for Global Environment Strategies (IGES), Hayama, Japan.
Joyce, J., Jewell, P.W., 2003. Physical controls on methane ebullition from reservoirs and lakes. Environ. Eng. Geosci. 9, 167–178.
Keller, M., Stallard, R.F., 1994. Methane emission by bubbling from Gatun Lake, Panama. J. Geophys. Res. 99, 8307–8319.
Laursen, A.E., Seitzinger, S.P., 2002a. Measurement of denitrification in rivers: an integrated, whole reach approach. Hydrobiologia 485, 67–81.
Laursen, A.E., Seitzinger, S.P., 2002b. The role of denitrification in nitrogen removal and carbon mineralization in Mid-Atlantic Bight sediments. Cont. Shelf Res. 22, 1397–1416.
MacIntyre, H.L., Kana, T.M., Geider, R.J., 2000. The effect of water motion on short-term rates of photosynthesis by marine phytoplankton. Trends Plant Sci. 5, 12–17.
Mattson, M.D., Likens, G.E., 1990. Air pressure and methane fluxes. Nature 347, 718–719.
McCutchan, J.H., Lewis, W.M., 2008. Spatial and temporal patterns of denitrification in an effluent-dominated plains river. Verh. Int. Ver. Limnol. 30, 323–328.
McCutchan, J.H., Saunders, J.F., Pribyl, A.L., Lewis Jr., W.M., 2003. Open-channel estimation of denitrification. Limnol. Oceanogr. Meth. 1, 74–81.
McCutcheon, S.C., Martin, J.L., Barnwell Jr., T.O., 1993. Water Quality. Handbook of Hydrology. McGraw-Hill, New York, NY.
McLinn, E.L., Stolzenburg, T.R., 2009. Ebullition-facilitated transport of manufactured gas plant tar from contaminated sediment. Environ. Toxicol. Chem. 28, 2298–2306.
Murphy, T., Lawson, A., Kumagai, M., Babin, J., 1999. Review of emerging issues in sediment treatment. Aquat. Ecosyst. Health Manage. 2, 419–434.
Ostrovsky, I., 2003. Methane bubbles in Lake Kinneret: quantification and temporal and spatial heterogeneity. Limnol. Oceanogr. 48, 1030–1036.
Pattinson, S.N., García-Ruiz, R., Whitton, B.A., 1998. Spatial and seasonal variation in denitrification in the Swale-Ouse system, a river continuum. Sci. Total Environ. 210/211, 289–305.
Poulin, P., Pelletier, E., Saint-Louis, R., 2007. Seasonal variability of denitrification efficiency in northern salt marshes: an example from the St. Lawrence Estuary. Mar. Environ. Res. 63, 490–505.
Pray, H.A., Schweickert, C.E., Minnich, B.H., 1952. Solubility of hydrogen, oxygen, nitrogen and helium in water. Ind. Eng. Chem. 44 (5), 1146–1151.

Pretty, U.N., Mason, C.F., Nedwell, D.B., Hine, R.E., Leaf, S., Dils, R., 2003. Environmental costs of freshwater eutrophication in England and Wales. Environ. Sci. Technol. 37, 201–208.

Pribyl, A.L., McCutchan, J.H., Lewis, W.M.J., Saunders, J.F.I., 2005. Whole-system estimation of denitrification in a plains river: a comparison of two methods. Biogeochemistry 73, 439–455.

Saunders, D.L., Kalff, J., 2001. Denitrification rates in the sediments of Lake Memphremagog, Canada–USA. Water Res. 35, 1897–1904.

Seitzinger, S., Harrison, J.A., BÖhlke, J.K., Bouwman, A.F., Lowrance, R., Peterson, B., Tobias, C., Van Drecht, G., 2006. Denitrification across landscapes and waterscapes: a synthesis. Ecol. Appl. 16, 2064–2090.

Seitzinger, S.P., 1988. Denitrification in freshwater and coastal marine ecosystems: ecological and geochemical significance. Limnol. Oceanogr. 33, 702–724.

Seitzinger, S.P., Nielsen, L.P., Caffret, J., Christensen, P.B., 1993. Denitrification measurement in aquatic sediment: a comparison of three methods. Biogeochemistry 23, 147–167.

Smith, L.K., Lewis Jr., W.M., 1992. Seasonality of methane emissions from five lakes and associated wetlands of the Colorado Rockies. Global Biogeochem. Cycles 6, 323–338.

State Environmental Protection Administration (SEPA), 2002. Environmental Quality Standards for Surface Water (GB3838-2002). State Environmental Protection Administration, Beijing, China, 12 pp. (in Chinese).

Takita, M., Sakamoto, M., 1993. Methane flux in a shallow eutrophic lake. Verh. Int. Ver. Limnol. 25, 822–826.

Teissier, S., Torre, M., 2002. Simultaneous assessment of nitrification and denitrification on freshwater epilithic biofilms by acetylene block method. Water Res. 36, 3803–3811.

Tortosa, G., David, C., Sánchez-Raya, A.J., Delgado, A., Sánchez-Monedero, M.A., Bedmar, E.J., 2011. Effects of nitrate contamination and seasonal variation on the denitrification and greenhouse gas production in La Rocina Stream (Doñana National Park SW Spain). Ecol. Eng. 37, 539–548.

Van Luijn, F., Boers, P.C.M., Lijklema, L., 1996. Comparison of denitrification rates in lake sediments obtained by the N_2 flux method, the 15N isotope pairing technique and the mass balance approach. Water Res. 30, 893–900.

Yan, W.J., Laursen, A.E., Andrew, E., Wang, F., Sun, P., Seitzinger, S.P., 2004. Measurement of denitrification in the Changjiang River. Envrion. Chem. 1, 95–98.

Zhong, J.C., Fan, C.X., Liu, G.F., Zhang, L., Shang, J.G., Gu, X.Z., 2010a. Seasonal variation of potential denitrification rates of surface sediment from Meiliang Bay, Taihu Lake, China. J. Environ. Sci. 22, 961–967.

Zhong, J.C., Fan, C.X., Zhang, L., Hall, E., Ding, S.M., Li, B., Liu, G.F., 2010b. Significance of dredging on sediment denitrification in Meiliang Bay China: a year long simulation study. J. Environ. Sci. 22, 68–75.